Hybrid Isolator for Mutual-Coupling Reduction in Millimeter-Wave MIMO Antenna Systems

MU'ATH AL-HASAN[1], (Member, IEEE), ISMAIL BEN MABROUK[2,3], (Member, IEEE), E'QAB R. F. ALMAJALI[4,5], (Member, IEEE), MOURAD NEDIL[3], (Senior Member, IEEE), AND TAYEB A. DENIDNI[6], (Fellow, IEEE)

[1]Department of Networks and Communication Engineering, Al Ain University of Science and Technology, Al Ain, United Arab Emirates
[2]Department of Networks and Communication Engineering, Al Ain University of Science and Technology, Abu Dhabi, United Arab Emirates
[3]Laboratoire de recherche Télébec en communications souterraines, Université du Québec en Abitibi-Témiscaminque, Val d'Or, QC J9X 5E4, Canada
[4]Department of Electrical and Computer Engineering, University of Sharjah, Sharjah, United Arab Emirates
[5]School of Electrical Engineering and Computer Science, University of Ottawa, Ottawa, ON K1N 6N5, Canada
[6]Centre Énergie Matériaux Télécommunications, INRS, Montreal, QC H2X 1E3, Canada

Corresponding author: Ismail Ben Mabrouk (ismail.mabrouk@aau.ac.ae)

ABSTRACT A novel millimeter-wave (MMW) hybrid isolator is presented to reduce the mutual-coupling (MC) between two closely-spaced dielectric resonators (DR) antennas at 60 GHz. The proposed hybrid isolator consists of a combination of a new uni-planar compact electromagnetic band-gap (EBG) structure and an MMW choke absorber. The design of the proposed EBG unit-cell is based on the stepped-impedance resonator (SIR) technique. The results show that the proposed EBG structure provides a wide frequency bandgap in the 60 GHz band with miniaturization factors of 0.79 and 0.66 compared to conventional uni-planar EBG and uni-planar compact (UC-EBG) structures, respectively. The proposed EBG is then placed between two Multiple-Input Multiple-Output (MIMO) DR antennas to reduce the MC level. As a result, an average of 7 dB level reduction is obtained. To further reduce the MC level, a thin MMW choke absorber wall is mounted vertically between the two DR antennas and above the EBG structure. An average of 22 dB MC reduction is achieved over the suggested bandwidth while maintaining good radiation characteristics. The measured isolation of the prototype antenna varies from –29 to –49 dB in the frequency range from 59.3 to 64.8 GHz. In fact, the proposed hybrid isolator outperforms other hybrid isolation techniques reported in the literature.

INDEX TERMS Millimeter-wave (MMW) antennas, dielectric resonator (DR) antennas, electromagnetic bandgap (EBG), mutual coupling (MC), multiple-input-multiple-output (MIMO) systems, choke absorber, stepped-impedance resonators (SIRs).

I. INTRODUCTION

With the recent advances in low-cost millimeter-wave (MMW) RF integrated circuits and devices, the use of MIMO techniques at frequencies as high as 60 GHz band has become very feasible as it satisfies the high bandwidth requirement of the emerging 5G wireless cellular networks and the associated advances in the Internet-of-Things (IoT) [1]–[3]. Given the rising channel capacity requirement for 5G, which is about 20 Gbps as proposed by the ITU [4], the most promising technique is to combine both the high bandwidth available at MMW bands, and the channel throughput improvement

achieved by exploiting the spatial degrees of freedom [5] to satisfy this soaring demand for data rate.

However, the mutual coupling MC between MIMO antennas at the 60 GHz band is found to be very significant and it deteriorates antennas' and propagation channel performance including array radiation pattern, side lobe level, gain, impedance matching of the radiating elements, and channel capacity [6]–[8].

In some applications, it is strictly required to have a MC level as low as −40 dB. In fact, in MIMO systems, it is required to keep low envelope correlation coefficient by keeping high isolation levels between radiating elements [9]. Therefore, isolation between antenna elements must be considered during the design stage of multiple antenna

---

The associate editor coordinating the review of this manuscript and approving it for publication was Chan Hwang See.

systems (MIMO), as this is crucial for reaching antenna-diversity schemes. In [10], [11] it was shown that the mutual coupling increases the channel correlation and reduces the radiation efficiency of the diversity antenna solution. Therefore, in order to obtain high diversity gain, the correlation between antenna ports must be minimized [12]. Moreover, driven by the recent deployment of 5G wireless systems, massive MIMO is considered as one of most promising technologies since it has shown over ten times channel capacity increase than a conventional MIMO system under realistic propagation scenarios. However, compact MIMO antennas are recommended in mobile terminals as well as in base stations (BS). Because of the close proximity of antenna elements, electromagnetic mutual coupling becomes inevitable [13]. The mutual coupling tends to alter the input impedance, reflection coefficients, and radiation patterns of the array elements. Thus, it is important to develop mutual coupling mitigation techniques from the antenna point of view.

Recently, several approaches have been reported to reduce MC effects and improve the isolation between radiating elements, such as slotted ground plane [14], [15], substrate integrated waveguides [16], frequency selective surfaces [11], [17], meta-materials [6], parasitic elements [18], neutralization lines [19], and Electromagnetic band-gap structures (EBG) [20].

Electromagnetic band-gap (EBG) structures are among the most used ways due its effectiveness and fabrication easiness. Mostly, EBG structures, when applied in MIMO antennas, are able to suppress surface waves by introducing frequency band-gaps where EM propagation is not allowed. For example, in [21], mushroom like EBG structure is incorporated in a 60 GHz dielectric resonator antenna to efficiently suppress surface waves from propagating by introducing an isolating bandgap over the suggested bandwidth. However, the presence of via holes and connections at MMW bands places severe constraints on the fabrication process and limits the potential applicability at these bands. Therefore, uni-planar EBG structures [22], [23], are more applicable and feasible at MMW bands. However, these structures (EBGs) are not efficient enough to suppress other main sources of MC, where its contribution to the isolation level is usually limited to surface wave suppression [21].

Consequently, hybrid isolation technique seems to be the best candidate to overcome other sources of MC. However, there is a paucity of research studies on hybrid isolators. In [24], a hybrid isolator composed of Mushroom EBG and two metallic chokes to reduce the mutual coupling between two patch antennas operating at 9.4 GHz, and an isolation improvement of about 13 dB was achieved.

In [25], a hybrid isolator is proposed to reduce mutual coupling between two microstrip antennas operating at 5.8 GHz. The hybrid isolator is realized by a metallic wall combined with two open-ended slots, and an isolation level of around -20 dB is achieved. Another hybrid approach to reduce MC is reported in [17], which involves frequency selective surface wall and two etched slots in the ground plane. Around -30 dB isolation level between two dielectric resonator (DR) antennas operating at the 60 GHz is achieved. In [7], the isolation level between two 60 GHz DR antennas varies between -30 dB to -47 dB. This is achieved by incorporating a metasurface comprising split ring resonators between DR elements.

In fact, the aforementioned hybrid isolators support the propagation of electric currents due to the existence of metallic structures. These currents affect the isolation level when coupled from one antenna to the other, hence, this affects MIMO antennas' radiation characteristics.

The scarcity of practical investigations on MC reduction at MMW bands can be mainly attributed to two reasons: First, the fabrication complexity and tolerance caused by the small physical spacing between the radiating elements, and therefore, the demand of a compact and easy-to-fabricate EBG structure to fit within the radiating elements becomes very challenging. Second, the wide bandwidths associated with MMW bands require isolators that work efficiently over a wide frequency bandwidth. Considering these factors and what other researchers achieved, this paper presents, an efficient hybrid isolator based on a combination of two isolation techniques by compacting uni planar EBG structure and a choke absorber. The design and miniaturization of the proposed EBG unit-cell is based on the stepped impedance resonator (SIR) technique [26]. The EBG miniaturization process is systematic and tunable to different frequency bands. Therefore, the main sources of MC can be controlled and considerably reduced without affecting the radiation characteristics by incorporating the proposed hybrid structure in MIMO antenna systems.

This paper is organized as follows. In section II, the theory and design considerations of the proposed hybrid isolator, which includes both an SIR-based miniaturized EBG structure and a choke absorber are presented. The MIMO antenna configuration considered in the design is also described in this section. Section III, presents an experimental validation of the proposed hybrid isolator in reducing the mutual coupling in MIMO antenna structure. Finally, the conclusion is drawn in Section IV.

II. PROPOSED HYBRID STRUCTURE

The MC level, in MIMO systems, depends mainly on the spacing between the radiating elements, the geometry and physical parameters of the antenna elements [11], [16], [17]. In planar antennas with common ground plane, the main sources of MC are surface waves propagating along the dielectric/air interface, space waves interacting in the near field region of the MIMO and hence increase coupling between different antenna elements and creeping waves propagating along the ground plane. Despite the no controlling of the creeping waves, both surface and space waves could be deliberately controlled to keep the MC under the desired level using the EBG unit-cell and the MMW choke absorber that are described in what follows.
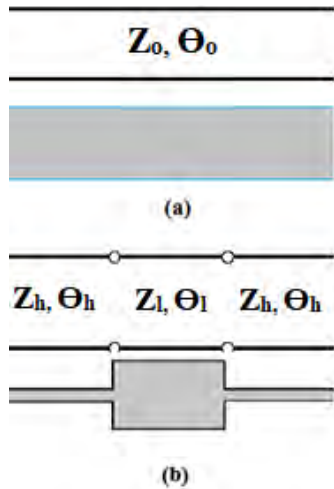
FIGURE 1. (a) Conventional EBG unit-cell and (b) its equivalent SIR configuration.
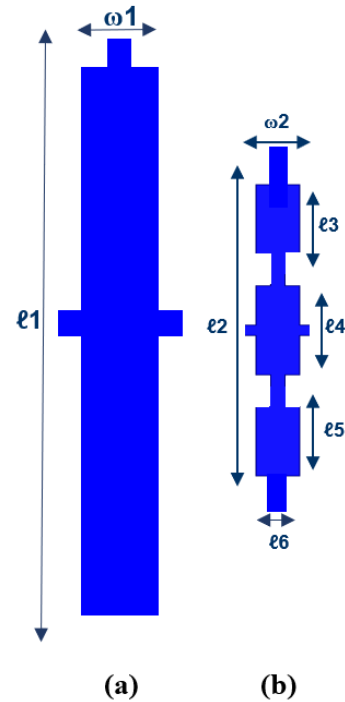

FIGURE 2. Layout of (a) conventional uni-planar EBG unit-cell and (b) proposed EBG unit-cell. The parameter values (all in millimeters) are: $\ell1 = 2.2$, w1 = 0.16, $\ell2 = 1.2$, w2 = 0.12, $\ell3 = 0.31$, $\ell4 = 0.40$, $\ell5 = 0.31$, and $\ell6 = 0.05$.

A. PROPOSED EBG UNIT-CELL

The proposed EBG unit-cell is designed and miniaturized based on the SIR technique. SIR technique is based on alternating sections of high and low characteristic impedance lines [26]. Due to their ease of design and compactness, SIR's are widely used in some applications where compactness is required.

The design procedure starts with a conventional uni-planar EBG unit cell, which will be referred to as "conventional EBG unit-cell" throughout this work, which consists of a single rectangular patch [22], as shown in FIGURE 1(a). The SIR equivalent of the conventional EBG unit-cell is shown in FIGURE 1(b), which will be referred to as "proposed EBG unit-cell" throughout this work is generated from the conventional unit cell with a miniaturization factor using the SIR technique. In order to have the conventional EBG unit-cell electrically equivalent to the proposed EBG unit-cell, the ABCD matrix of the conventional EBG unit-cell [26], must be equal to the product of the ABDC matrices of the Hi-Z, Low-Z, Hi-Z of the SIR EBG unit-cell, i.e.,

$$
\begin{bmatrix} cos\theta_o & jZ_o sin\theta_o \\ j\dfrac{1}{Z_o} sin\theta_o & cos\theta_o \end{bmatrix}
$$
$$
= \begin{bmatrix} cos\theta_h & jZ_h sin\theta_h \\ j\dfrac{1}{Z_h} sin\theta_h & cos\theta_h \end{bmatrix} \begin{bmatrix} cos\theta_l & jZ_l sin\theta_l \\ j\dfrac{1}{Z_l} sin\theta_l & cos\theta_l \end{bmatrix}
$$
$$
\times \begin{bmatrix} cos\theta_h & jZ_h sin\theta_h \\ j\dfrac{1}{Z_h} sin\theta_h & cos\theta_h \end{bmatrix} \quad (1)
$$

matrix multiplications and rearrangement yield:

$$
cos\theta_l = \frac{cos\theta_o \left(1 - K^2 tan^2 (\theta_h)\right) + \frac{1}{M} sin\theta_o \left(1 + K^2\right) tan\theta_h}{1 + K^2 tan^2 (\theta_h)} \quad (2)
$$

where

$$
\theta = \beta l, \quad K = tan\theta_l tan\theta_h = \frac{Z_h}{Z_l} \text{ and } M = tan\theta_o tan\theta_h = \frac{Z_h}{Z_o}
$$

The miniaturization factor [27], is given by:

$$
\frac{2\theta_h + \theta_l}{\theta_0} \quad (3)
$$

Therefore, by choosing the proper values of the line impedances **Zh** and **Zℓ** and the electrical lengths **Θh** and **$\Theta\ell$**, it can be shown that both configurations can have the same ABCD matrices with a miniaturization factor that depends on the values of **Θh** and **$\Theta\ell$**. However, the physical dimensions of the proposed EBG unit-cell are less than that of the conventional one.

The parameters' values of the proposed EBG unit-cell were chosen based on equations (1−3) and further optimized using CST simulator [28].

FIGURE 2 shows a layout of the conventional and proposed EBG unit-cells. Both the conventional and proposed EBG structures were printed on the top of a 0.25 mm thick ROGERS RO3006 substrate.

The proposed EBG unit-cell consists of three rectangular patches connected through narrow metallic branches in the vertical direction. Both conventional and proposed unit-cells are connected to adjacent cells through connecting bridges in both directions.

Using equations (1-3), the calculated miniaturization factor for the proposed EBG unit-cell is 0.79. The physical areas of

the conventional and proposed EBG unit-cells are 2.64 mm^2 and 1.92 mm^2, respectively, with a miniaturization factor of 0.73. Both miniaturization factors are well matched with each other.

FIGURE 3 shows the simulated transmission coefficients of the proposed and conventional EBG unit-cells. Simulations were carried out using CST simulator. It is apparent that both conventional and proposed EBG unit-cells have similar transmission coefficients. Both unit-cells have a bandgap around the 60 GHz frequency band, with a transmission coefficient of less than −50 dB. This indeed confirms the validity of the SIR technique in generating a manituraized EBG unit-cell from a conventional one without degrading the performance.
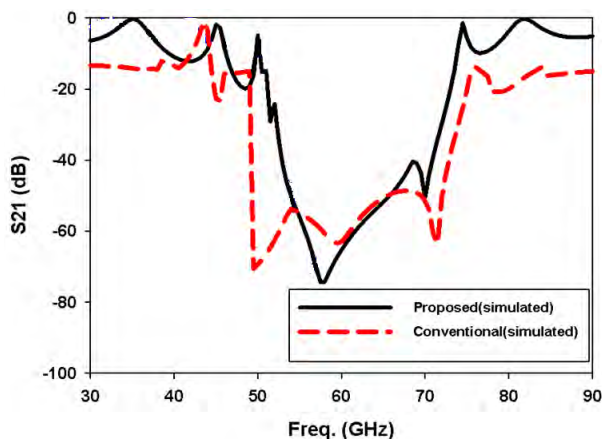
FIGURE 3. Simulated transmission coefficients of the proposed and conventional EBG structures.

In order to further examine the transmission characteristics of the proposed EBG unit-cell, the dispersion diagram is calculated using CST software.

The dispersion diagram of any EBG unit-cell usually shows the propagating modes versus the wave number over the irreducible Brillouin zone (the **Γ-X-M** region shown inside the red triangle shown in FIGURE 4) for different phases. The irreducible Brillouin zone is defined as the minimum area required to construct the EBG unit-cell [29].

Since the proposed EBG unit-cell is asymmetric along the irreducible Brillouin zone, one can expect different bandgaps for the different **Γ-X**, **X-M**, and **M- Γ** directions. However, only guided modes propagating through the proposed EBG unit-cell along the **Γ-X** will be examined in the next section. These modes can be determined by varying the phase difference along the **Γ-X** direction from 0 to pi radians, while keeping the phase difference along the **X-M** direction at a constant value of 0 radians. This results in a region above the light line, in which no EM wave propagation is allowed.

FIGURE 4 shows the dispersion diagram of the proposed EBG unit-cell. The figure shows the first two propagating modes (solid and dotted lines, respectively). The two vertical lines represent the light line. Results show a bandgap between the first two propagating modes for different wave numbers along the **Γ-X** direction and in the region above the light

line. The proposed EBG has a bandgap from 56.8 GHz to 66.6 GHz, with a gap to mid-gap ratio of 14.8% over the **Γ-X** direction. This agrees well with the results previously highlighted in FIGURE 3. Over this frequency band, electromagnetic waves with different phases are prohibited from propagating along this direction.
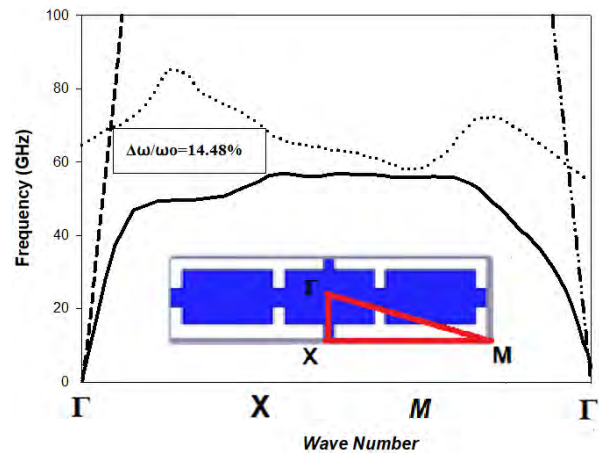
FIGURE 4. Dispersion diagram of the proposed EBG unit-cell.

B. MMW CHOKE ABSORBER

The 0.5 mm thick MS−760KW absorber from Epoch Microelectronics [30], which is used in the hybrid structure, is shown in FIGURE 5(a). This absorber is designed using silicone gel binder. The filler particle composition in the absorber yields suppression of unwanted EM energy coupling and surface currents. In addition, it provides consistent performance due to temperature stability. The attenuation performance of the MS−760KW absorber is shown in FIGURE 5(b). As shown, the selected absorber has an attenuation performance of less than −20 dB around the 60 GHz band.

The purpose of the absorber is to reduce coupling between higher order modes in the reactive near-field region between the two Dielectric Resonator antennas (DR) of the MIMO configuration described in the next section.

C. MIMO ANTENNA CONFIGURATION

The layout of the MIMO antenna is shown in FIGURE 6. It consists of two identical aperture-coupled DR antennas mounted on the top of 0.25 mm thick ROGERS 3006 substrate. The spacing between the antenna elements is half of the free space wavelength at 60 GHz which corresponds to 2.5 mm. The diameter and height of the DR antenna are 1.06 mm and 1.27 mm, respectively. The DR antennas are fed by two identical 50 Ω microstrip lines of 0.36 mm width, each. The microstrip lines are printed on a 0.25 mm thick ROGERS 3006 substrate. The energy is coupled to the DR antennas through two identical slots etched in the ground plane.
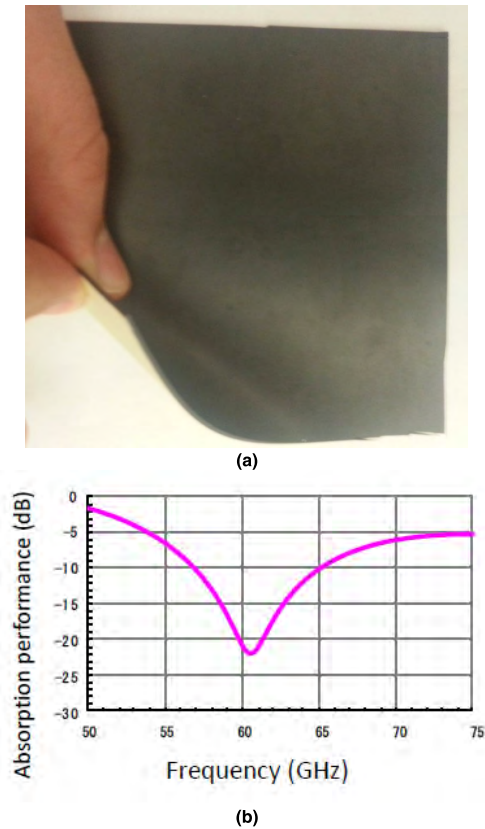
(a)

(b)

FIGURE 5. (a) The MS-760KW absorber and (b) the absorption performance (as taken from the data sheet).
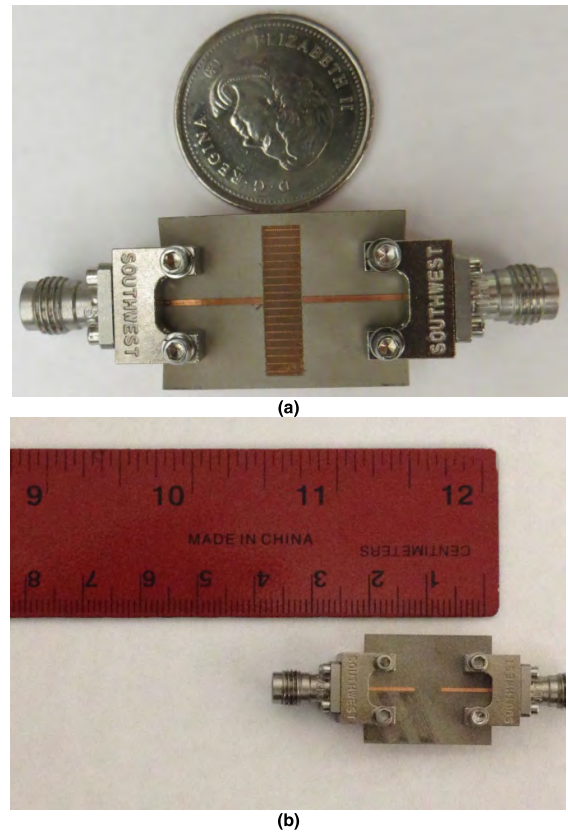

(a)

(b)

FIGURE 7. (a) The fabricated symmetric microstrip line structure and (b) the reference structure.
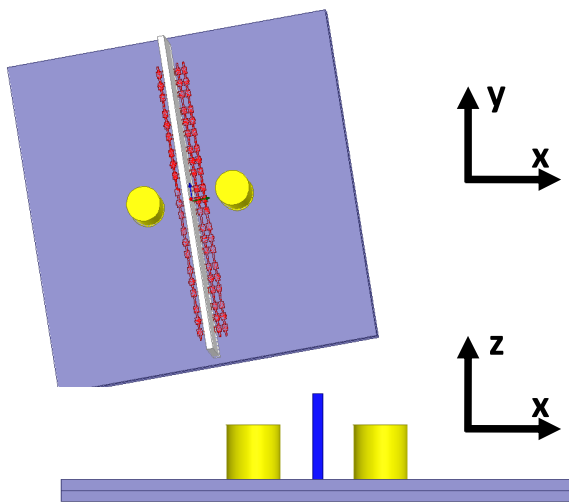

FIGURE 6. Layout of the DR antennas: Perspective view (top) and side view (bottom).

Slot-coupling has the advantage of isolating the microstrip feedline from the DR antennas. However, at MMW bands, the dimensions of the feed line are comparable to those of the radiating elements [7]. The slot has a length and width of 0.87 mm and 0.18 mm, respectively.

Five periods of the proposed EBG structure were interposed between the two radiating elements. Finally,

1.0 ~ 1.1 mm high and 0.5 mm thick choke absorber was vertically added and mounted between these two radiating elements.

III. VALIDATION AND EXPERIMNETAL RESULTS
A. MEASURED TRANSMISSION COEFFICIENT FOR THE EBG UNIT-CELL

The transmission coefficient of the proposed EBG unit-cell was measured using the symmetric microstrip line technique [21], for the fabricated EBG unit-cell shown in FIGURE 7(a).

In the microstrip line technique, a lattice of the proposed EBG is inserted between two open ended, symmetric 50 Ω microstrip lines of width 0.36 mm printed on the top of 0.25 mm thick ROGERS RO3006 substrate. Electromagnetic waves are launched by the first microstrip line, and detected by the second microstrip line. The transmission coefficient is then measured and compared to the transmission coefficient measured for a reference structure, which includes two identical open ended microstrip lines but with the absence of any EBG lattice in the middle, as shown in FIGURE 7(b). Consequently, the attenuation due to the conductor and dielectric losses will be the same in both structures, and hence, any difference in the transmission characteristics will be solely attributed to the EBG structure.

The microstrip line technique reduces the influence of parasitic modes and as a single-layer technique, it has the advantage of ease of fabrication as compared to the two layers suspended microstrip line technique [31].

FIGURE 8(a) shows a microscopic photo of the fabricated EBG structure used in the measurements. Measured and simulated transmission coefficients of the proposed EBG structure are shown in FIGURE 8(b). The measured and simulated transmission coefficients ties very well. The VNA used for this measurement goes up to 65 GHz hence, measured results stop at 65 GHz.
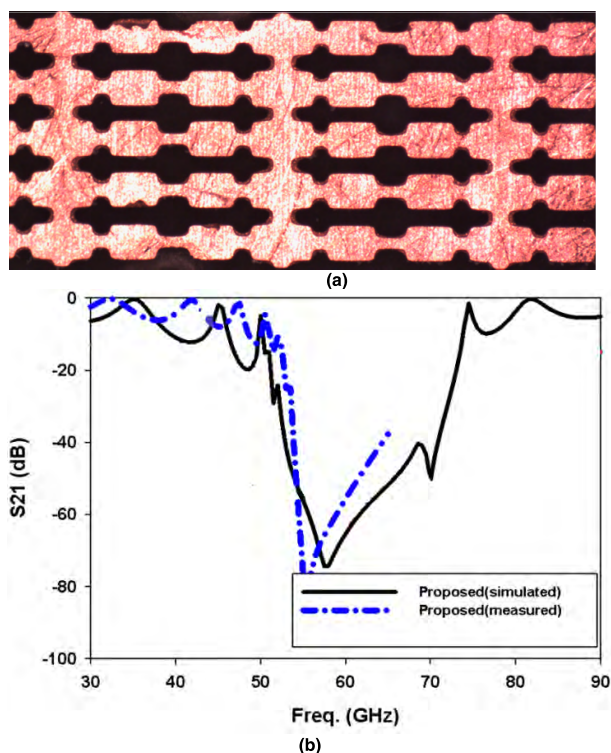
(a)

(b)

FIGURE 8. (a) Fabricated EBG unit-cell and (b) measured and simulated transmission coefficients of the proposed EBG structures.

B. EXPERIMENTAL RESULTS FOR THE FABRICATED MIMO

In order to demonstrate the ability and performance of the proposed hybrid isolator, three MIMO antenna prototypes were fabricated and tested as shown in FIGURE 9. The three fabricated prototypes are: the reference MIMO antenna without EBG structure or choke absorber shown in FIGURE 9(a), the MIMO antenna with EBG structure shown in FIGURE 9(b), and the hybrid MIMO antenna with both EBG structure and choke absorber shown in FIGURE 9(c). The choke absorber was rubbed against a piece of sand paper to elaborate the required height and thickness.

The absorber choke is mainly used to mitigate the EM interactions caused by the space waves [26]. On the other hand, the EBG structure is presented to improve the isolation level through controlling surface-waves propagation [21].
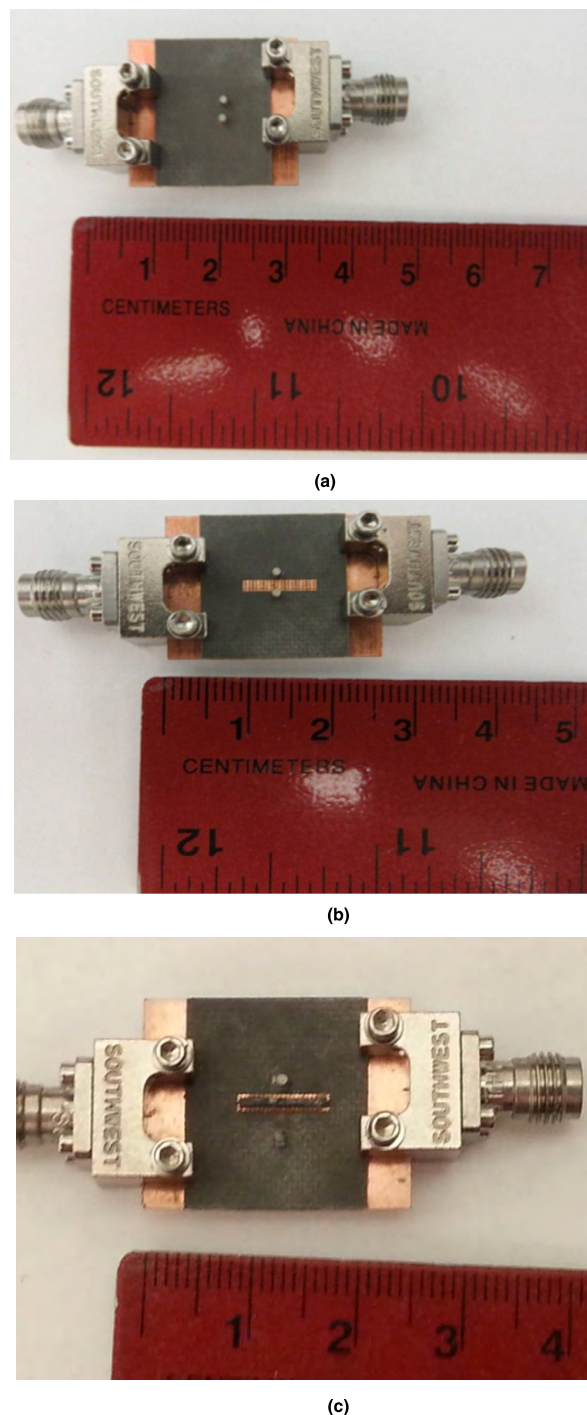
(a)

(b)

(c)

FIGURE 9. Photos for the fabricated antenna array prototypes: (a) reference DR antennas, (b) DR antennas with EBG structure, and (c) DR antennas with the proposed hybrid isolator (EBG structure and choke absorber).

Therefore, by combining both isolation techniques, sources of MC could considerably be controlled and reduced.

FIGURE 10 exhibits the measured transmission coefficient for all prototypes shown in FIGURE 9. The MIMO antenna prototype with EBG structure yields around 5 to 13 dB isolation improvement over the reference
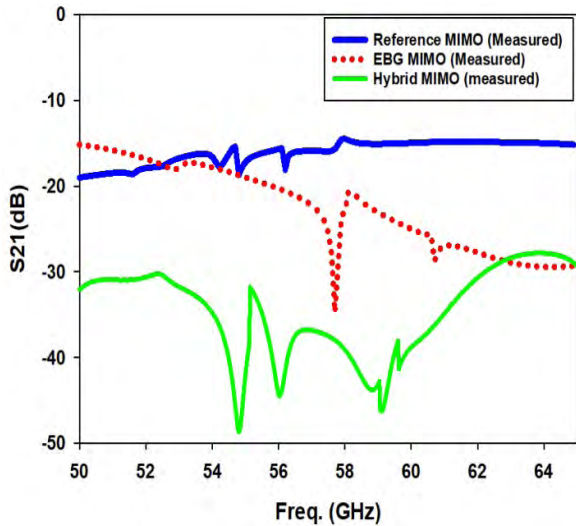
FIGURE 10. Measured transmission coefficients of the reference, EBG, and hybrid MIMO antenna prototypes.

MIMO antenna prototype. The average reduction, as compared to the reference prototype results, is close to 10 dB in a quit broad frequency band (54 GHz-65 GHz). On the other hand, the hybrid MIMO antenna has an isolation enhancement of about 25 dB over the reference MIMO antenna, and about 10 dB over the MIMO antenna prototype with EBG only. The choke absorber is located in the reactive near-filed region of the radiating elements. In this region, a strong coupling exists due to the higher order modes (evanescent modes) and the interaction between surface currents. This justifies the significant isolation level improvement once the choke absorber is incorporated. Table 1 summarizes the results.

TABLE 1. Summary of the transmission coefficients for different isolation techniques.

Isolation Technique	Average Mutual-coupling level reduction
Reference Array(no isolation)	16 dB
EBG Isolator	21-29 dB
Proposed Hybrid Isolator	30-40 dB

FIGURE 11 shows the measured reflection coefficients of the three MIMO antenna prototypes. The three MIMO antenna prototypes are well matched over the desired frequency bandwidth ($S_{11} < -10\ dB$). However, the presence of the EBG structures in both: MIMO antenna prototype with EBG and the hybrid antenna prototype, negatively affect the impedance matching level. In fact, EBGs are resonant structures, which have high equivalent impedance at resonance, therefore, when placed close to the DR antenna elements, they alter the input impedance of the antenna structure and consequently, impacts the impedance matching.

An electrically-long microstrip feed-lines are needed to accommodate the connectors. This tends to decrease the radiation efficiency of the MIMO prototype.
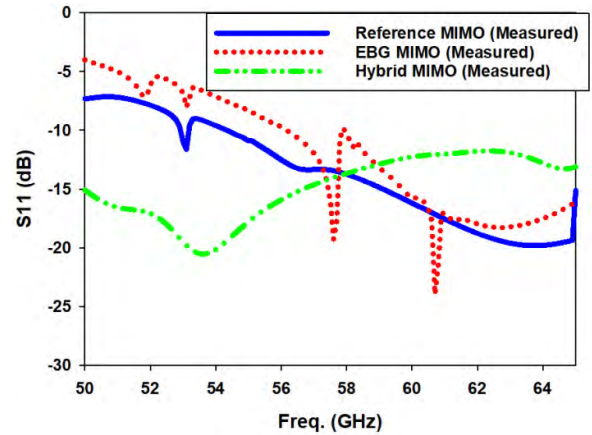

FIGURE 11. Measured reflection coefficients of the reference, EBG, and hybrid MIMO antenna prototypes.
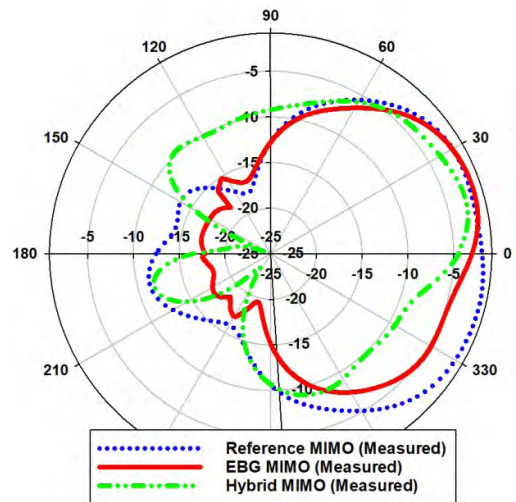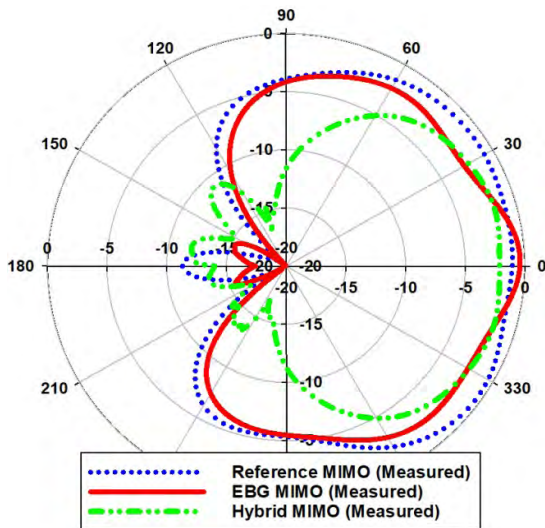

FIGURE 12. Normalized H-plane ($\phi = 0°$) radiation patterns of DR antenna element for different isolation techniques.

The calculated-from-measured radiation efficiency of the hybrid MIMO antenna prototype is 69%, at 60 GHz.

FIGURES 12 and 13 show the normalized measured H- and E- plane radiation patterns at 60 GHz for a single DR antenna element for different isolation techniques, respectively. The measurements were carried out with one microstrip feed line which is excited while the other microstrip feed line is terminated with a matched load. It can be observed from FIGURE 12 that the H-plane radiation patterns experienced some changes when the EBG isolator and the hybrid isolator are used. The H-plane radiation pattern for the EBG MIMO has around 5 dB reduction along the substrate edges (90° and 270°) as compared to the reference one. This is due to the ability of the EBG structure to block surface wave propagation. On the other hand, the main peak direction in the H-plane is tilted by about 30° from the broadside direction for the hybrid MIMO prototype. This is resulted from the presence of the choke absorber. The front to back

FIGURE 13. Normalized E-plane ($\phi = 0o$) radiation patterns of DR antenna element for different isolation techniques.

ratio is improved for the EBG MIMO and the Hybrid MIMO due to the reduction of the edge scattering effect. As for the E-plane patterns, it is evident that all E-plane pattern have their maximum radiation level in the broadside direction.

The gain of the reference and hybrid MIMO antenna prototypes is calculated from the gain of a single DR element and using the antennas theory. The calculated gain value (from measured patterns) of the hybrid MIMO prototype is 8.1 dBi at 60 GHz with 1.9 dBi enhancement over the reference MIMO antenna. In addition, the back radiation is noticeably reduced.

The E-plane radiation patterns of the MIMO antenna with EBG and hybrid MIMO antenna are narrower than that of the references MIMO antenna. In fact, the existence of the EBG structure reduces edge diffraction and minimizes backward radiation.

IV. CONCLUSIONS

In this paper, new EBG unit-cell and hybrid isolator operating at the 60 GHz band have been proposed and investigated. The new EBG unit-cell is realized by miniaturized a uni-planar EBG structure. The EBG structure is miniaturized based on the stepped impedance resonator technique. The miniaturization process is systematic and tunable to different frequency bands hence, it can be used by other researchers to design EBG unit-cells. The transmission characteristics of the proposed EBG structure show a wide bandgap around the 60 GHz frequency band as compared to a reference model that does not include the proposed EBG unit-cell. The EBG unit cell was tested in a MIMO antenna, which comprises of two DR antenna elements, and has shown its effectiveness in reducing the unwanted mutual coupling between the MIMO elements. The hybrid isolator is then incorporated by adding a choke absorber to the EBG unit cell to further reduce the mutual coupling between closely-spaced dielectric

resonator MIMO antenna systems. Experimental results show the potential and capability of this hybrid isolator in reducing the MC level and enhancing the isolation. This efficient isolator is expected to be very useful for massive MIMO for 5G wireless communication systems.

REFERENCES

[1] A. Dadgarpour, M. S. Sorkherizi, A. A. Kishk, and T. A. Denidni, "Single-element antenna loaded with artificial mu-near-zero structure for 60 GHz MIMO applications," *IEEE Trans. Antennas Propag.*, vol. 64, no. 12, pp. 5012–5019, Dec. 2016.

[2] R. Hussain, A. T. Alreshaid, S. K. Podilchak, and M. S. Sharawi, "Compact 4G MIMO antenna integrated with a 5G array for current and future mobile handsets," *IET Microw., Antennas Propag.*, vol. 11, no. 2, pp. 271–279, 2017.

[3] R. Tian, Y. Liang, X. Tan, and T. Li, "Overlapping user grouping in IoT oriented massive MIMO systems," *IEEE Access*, vol. 5, pp. 14177–14186, 2017.

[4] *Possible Network Parameters on IMT-2020/5G Transport Network*, Int. Telecommun. Union, Tokyo, Japan, 2017.

[5] W. Lv, R. Wang, J. Wu, J. Xu, P. Li, and J. Dou, "Degrees of freedom of the circular multirelay MIMO interference channel in IoT networks," *IEEE Internet Things J.*, vol. 5, no. 3, pp. 1957–1966, Jun. 2018.

[6] M. Farahani, J. Pourahmadazar, M. Akbari, M. Nedil, A. R. Sebak, and T. A. Denidni, "Mutual coupling reduction in millimeter-wave MIMO antenna array using a metamaterial polarization-rotator wall," *IEEE Antennas Wireless Propag. Lett.*, vol. 16, pp. 2324–2327, 2017.

[7] A. Dadgarpour, B. Zarghooni, B. S. Virdee, T. A. Denidni, and A. A. Kishk, "Mutual coupling reduction in dielectric resonator antennas using metasurface shield for 60-GHz MIMO systems," *IEEE Antennas Wireless Propag. Lett.*, vol. 16, pp. 477–480, 2017.

[8] H. Qi, L. Liu, X. Yin, H. Zhao, and W. J. Kulesza, "Mutual coupling suppression between two closely spaced microstrip antennas with an asymmetrical coplanar strip wall," *IEEE Antennas Wireless Propag. Lett.*, vol. 15, pp. 191–194, 2016.

[9] T. J. Douglas and K. Sarabandi, "A high-isolation two-port planar antenna system for communication and radar applications," *IEEE Access*, vol. 6, pp. 9951–9959, 2018.

[10] D. Lu, L. Wang, E. Yang, and G. Wang, "Design of high-isolation wideband dual-polarized compact MIMO antennas with multiobjective optimization," *IEEE Trans. Antennas Propag.*, vol. 66, no. 3, pp. 1522–1527, Mar. 2018.

[11] S. R. Thummaluru, R. Kumar, and R. K. Chaudhary, "Isolation enhancement and radar cross section reduction of MIMO antenna with frequency selective surface," *IEEE Trans. Antennas Propag.*, vol. 66, no. 3, pp. 1595–1600, Mar. 2018.

[12] I. Ben Mabrouk, J. Hautcoeur, L. Talbi, M. Nedil, and K. Hettak, "Feasibility of a millimeter-wave MIMO system for short-range wireless communications in an underground gold mine," *IEEE Trans. Antennas Propag.*, vol. 61, no. 8, pp. 4296–4305, Aug. 2013.

[13] X. Chen, S. Zhang, and Q. Li, "A review of mutual coupling in MIMO systems," *IEEE Access*, vol. 6, pp. 24706–24719, 2018.

[14] J. Deng, J. Li, L. Zhao, and L. Guo, "A dual-band inverted-F MIMO antenna with enhanced isolation for WLAN applications," *IEEE Antennas Wireless Propag. Lett.*, vol. 61, pp. 2270–2273, 2018.

[15] J.-Y. Deng, L.-X. Guo, and X.-L. Liu, "An ultrawideband MIMO Antenna with a high isolation," *IEEE Antenna Wireless Propag. Lett.*, vol. 15, pp. 182–185, 2016.

[16] C. Lee, M. K. Khattak, and S. Kahng, "Wideband 5G beamforming printed array clutched by LTE-A 4×4-multiple-input–multiple-output antennas with high isolation," *IET Microw., Antennas Propag.*, vol. 12, no. 8, pp. 1407–1413, 2018.

[17] R. Karimian, A. Kesavan, M. Nedil, and T. A. Denidni, "Low-mutual-coupling 60-GHz MIMO antenna system with frequency selective surface wall," *IEEE Antennas Wireless Propag. Lett.*, vol. 16, pp. 373–376, 2017.

[18] Z. Li, Z. Du, M. Takahashi, K. Saito, and K. Ito, "Reducing mutual coupling of MIMO antennas with parasitic elements for mobile terminals," *IEEE Trans. Antennas Propag.*, vol. 60, no. 2, pp. 473–481, Feb. 2012.

[19] S. Zhang and G. F. Pedersen, "Mutual coupling reduction for UWB MIMO antennas with a wideband neutralization line," *IEEE Antennas Wireless Propag. Lett.*, vol. 15, pp. 166–169, 2016.

[20] M. J. Al-Hassan, ''Millimeter-wave electromagnetic band-gap structures for antenna and antenna arrays applications,'' Ph.D. dissertation, Dept. Energy Mater. Telecommun., Univ. Québec, Montreal, QC, Canada, 2015.

[21] M. J. Al-Hasan, T. A. Denidni, and A. Sebak, ''Millimeter-wave EBG-based aperture-coupled dielectric resonator antenna,'' *IEEE Trans. Antennas Propag.*, vol. 61, no. 8, pp. 4354–4357, Aug. 2013.

[22] S. K. Sharma and L. Shafai, ''Enhanced performance of an aperture-coupled rectangular microstrip antenna on a simplified unipolar compact photonic band gap (UC-PBG) structure,'' in *Proc. IEEE Antennas Propag. Soc. Int. Symp.*, vol. 2, Jul. 2001, pp. 498–501.

[23] R. Coccioli, F.-R. Yang, K.-P. Ma, and T. Itoh, ''Aperture-coupled patch antenna on UC-PBG substrate,'' *IEEE Trans. Microw. Theory Techn.*, vol. 47, no. 11, pp. 2123–2130, Nov. 1999.

[24] M. Niroo-Jazi, T. A. Denidni, M. R. Chaharmir, and A. R. Sebak, ''A hybrid isolator to reduce electromagnetic interactions between Tx/Rx antennas,'' *IEEE Antennas Wireless Propag. Lett.*, vol. 13, pp. 75–78, 2014.

[25] H. Qi, X. Yin, and H. Zhao, ''A hybrid solution for mutual coupling reduction between closely spaced microstrip antennas,'' in *Proc. Asia–Pacific Microw. Conf. (APMC)*, vol. 5, Dec. 2015, pp. 1–3.

[26] M. D. Pozar, *Microwave Engineering*, 4th ed. Hoboken, NJ, USA: Wiley, 2011.

[27] B. Zarghooni and T. A. Denidni, ''New compact metamaterial unit-cell using SIR technique,'' *IEEE Microw. Wireless Compon. Lett.*, vol. 24, no. 5, pp. 315–317, May 2014.

[28] *Microwave Studio*. Accessed: Jan. 1, 2019. [Online]. Available: www.cst.com

[29] F. Yang and Y. Rahmat-Samii, *Electromagnetic Band Gap Structures in Antenna Engineering*. Cambridge, U.K.: Cambridge Univ. Press, 2008.

[30] *Epoch Microelectronics*. Accessed: Jan. 1, 2019. [Online]. Available: www.epochmicro.com

[31] O. Ayop and M. K. A. Rahim, ''Analysis of mushroom-like electromagnetic band gap structure using suspended transmission line technique,'' in *Proc. IEEE Int. RF Microw. Conf.*, Dec. 2011, pp. 258–261.

MU'ATH AL-HASAN received the B.A.Sc. degree in electrical engineering from the Jordan University of Science and Technology, Jordan, in 2005, the M.A.Sc. degree in wireless communications from Yarmouk University, Jordan, in 2008, and the Ph.D. degree in telecommunication engineering from the Institut National de la Recherche Scientifique (INRS), Universitédu Québec, Montreal, QC, Canada, in 2015. In 2015, he joined Concordia University as a Postdoctoral Fellow. He is currently an Assistant Professor with the Al Ain University of Science and Technology, Abu Dhabi, United Arab Emirates. His current research interests include MMW antennas, Multiple-Input and Multiple-Output (MIMO) systems, electromagnetic bandgap (EBG) structures, and frequency selective surfaces (FSS).

ISMAIL BEN MABROUK received the B.A.Sc. and M.A.Sc. degrees in electrical engineering from the University of Lille, Lille, France, in 2006 and 2007, respectively, and the Ph.D. degree in electrical engineering from the University of Quebec, Canada, in 2012. From 2007 to 2009, he was with Huawei Technologies, Paris, France. In 2012, he joined the Wireless Devices and Systems (WiDeS) Group at University of Southern California, Los Angeles, CA, USA. He is currently an Assistant Professor with the Al Ain University of Science and Technology, Abu Dhabi, UAE, and also an Adjunct Professor with the Université de Québec en Abitibi-Témiscamingue. His research activities include propagation studies for Multiple-Input and Multiple-Output (MIMO) systems, measurement campaigns in special environments, WBAN, and antenna design at the MMW and THz frequencies.

E'QAB R. F. ALMAJALI received the B.Sc. degree (Hons.) from Mu'tah University, Jordan, in 2003, and the M.A.Sc. and Ph.D. degrees (Hons.) from the University of Ottawa, Ottawa, ON, Canada, in 2010 and 2014, respectively, all in electrical engineering.

He was a Postdoctoral Fellow with the Electronics Department, Carleton University, Canada. He has been an Assistant Professor with the Electrical Engineering Department, University of Sharjah, since 2018. He is also an Adjunct Professor with the University of Ottawa. He is an author of over 30 technical publications and a coauthor of a book chapter on *reflect array antennas* (Artech, 2013). His current research interests and activities include periodic structures, frequency selective surfaces, 5G high-gain MIMO antennas, transmit arrays, and low profile holographic antennas.

Dr. Almajali was a recipient of the NSERC-PGS Scholarship for his doctoral studies, in 2012, and the Prestigious Canadian National Science and Engineering Research Council (NSERC) Postdoctoral Fellowship for his research excellence, in 2014.

MOURAD NEDIL (M'08–SM'12) received the Dipl.-Ing. degree from the University of Algiers, Algiers, Algeria, in 1996, the D.E.A. (M.S.) degree from the University of Marne la Vallée, Marne la Vallée, France, in 2000, and the Ph.D. degree from the Institut National de la Recherche Scientifique (INRS-EMT), Université de Québec, Montreal, QC, Canada, in 2006. He received the Postdoctoral Fellowship from the RF Communications Systems Group, INRS-EMT, from 2006 to 2008. In 2008, he joined the Engineering School Department, Université de Québec en Abitibi-Témiscamingue, Rouyn-Noranda, QC, Canada, where he is currently an Associate Professor. His current research interests include antennas, multiple-input and multiple-output radio-wave propagation, and microwave devices.

TAYEB A. DENIDNI (M'98–SM'04–F'19) received the M.Sc. and Ph.D. degrees in electrical engineering from Laval University, Quebec, QC, Canada, in 1990 and 1994, respectively.

From 1994 to 2000, he was a Professor with the Engineering Department, Université du Quebec in Rimouski (UQAR), Rimouski, QC, Canada, where he founded the Telecommunications Laboratory. Since 2000, he has been with the Institut National de la Recherche Scientifique (INRS), University of Quebec, Montreal, QC, Canada. He founded the RF Laboratory, INRS- Energie, Materiaux et Telecommunications (INRS-EMT), Montreal. He has extensive experience in antenna design. He served as a Principal Investigator on many research projects sponsored by NSERC, FCI, and numerous industries. His current research interests include reconfigurable antennas using electromagnetic bandgap and frequency-selective surface structures, dielectric resonator antennas, meta-material antennas, adaptive arrays, switched multi-beam antenna arrays, ultra wide-band antennas, microwave, and development for wireless communications systems.

• • •